Matrix Isolation Infrared Spectroscopic and Theoretical Study of Group IV Metal Oxide Clusters: M_2O_2 and M_2O_4

Yu Gong, QingQing Zhang, and Mingfei Zhou*

Department of Chemistry, Shanghai Key Laboratory of Molecular Catalysts and Innovative Materials, Advanced Materials Laboratory, Fudan University, Shanghai 200433, P.R. China

Received: February 9, 2007; In Final Form: March 9, 2007

Dinuclear titanium, zirconium, and hafnium oxide clusters, M_2O_2 and M_2O_4 (M = Ti, Zr, Hf) have been prepared and characterized by matrix isolation infrared spectroscopy and quantum chemical calculations. The M_2O_2 clusters were formed through the reactions of metal dimers and O_2 in solid argon upon sample annealing. Theoretical calculations indicate that the Ti_2O_2 cluster has a singlet ground state with a nonplanar cyclic C_{2v} structure with a strong Ti−Ti bond, while the Zr_2O_2 and Hf_2O_2 clusters have planar cyclic structures. The M_2O_4 clusters were characterized to have a closed-shell singlet ground state with a nonplanar C_{2h} symmetry, which were formed from the dimerization of the metal dioxide molecules.

Introduction

Group IV metal oxides are widely used as catalysts and catalytic supports in many important chemical processes.[1] The simple metal oxide clusters serve as interesting models in understanding the nature of active species in catalysis at the molecular level. Numerous studies have been devoted to the investigation of the electronic and geometric structures and reactivities of group IV metal oxide molecules and small clusters.[2−23] The metal monoxide and dioxide molecules produced either by thermal evaporation of bulk oxides or reaction between metal atoms and oxygen were investigated spectroscopically in the gas phase as well as in solid noble-gas matrixes.[2−9] Metal oxide clusters can easily be generated in a supersonic expansion by laser ablation of the metal and reaction with dioxygen. Mass spectra of the neutral oxide clusters were obtained by laser photoionization.[10,11] The M_xO_{2x} and M_xO_{2x+1} clusters (M = Ti, Zr) were found to be the most stable neutral clusters for high oxygen content in the expansion gas, while oxygen deficient clusters were observed in low oxygen content. The electronic structures of titanium oxide clusters, $(TiO_2)_n$ (n = 1−4) were studied by anion photoelectron spectroscopy.[7] The $(TiO_2)_n$ clusters (n = 2, 3, 4) are all closed-shell, with HOMO−LUMO gaps similar to that of TiO_2 and with increasing electron affinities. The vibrational properties of the $(Ti_2O_3)_x(TiO_2)_y$ with (x,y) from (2,4) to (11,29) and Zr_nO_{2n-1} clusters were obtained using infrared resonance enhanced multiphoton ionization spectroscopy.[12,13] The electronic structure and stability of group IV metal oxide clusters, particularly small titanium oxide clusters, have also been intensively studied by various theoretical methods.[14−22]

In this paper, we present a matrix isolation infrared spectroscopic study on M_2O_2 and M_2O_4 to further understand the structure and chemical bonding between group IV metal and oxygen. These small metal oxide clusters are fundamental building blocks for the formation of large metal oxide clusters.

Experimental and Computational Methods

The M_2O_2 and M_2O_4 clusters were produced by the reactions of laser-evaporated metal atoms and dimers with dioxygen in solid argon. The experimental setup for pulsed laser-evaporation and matrix isolation infrared spectroscopic investigation has been described in detail previously.[24] Briefly, the 1064 nm fundamental of a Nd:YAG laser (Continuum, Minilite II, 10 Hz repetition rate and 6 ns pulse width) was focused onto a rotating metal target through a hole in a CsI window cooled normally to 6 K by means of a closed-cycle helium refrigerator (ARS, 202N). The laser-evaporated metal atoms were co-deposited with oxygen/argon mixtures onto the CsI window. In general, matrix samples were deposited for 1−1.5 h at a rate of 4 mmol/h. The O_2/Ar mixtures were prepared in a stainless steel vacuum line using standard manometric technique. Isotopic $^{18}O_2$ (ISOTEC, 99%) was used without further purification. The infrared absorption spectra of the resulting samples were recorded on a Bruker IFS 66V spectrometer at 0.5 cm^{-1} resolution between 4000 and 450 cm^{-1} using a liquid nitrogen cooled HgCdTe (MCT) detector.

Quantum chemical calculations were performed using the Gaussian 03 program.[25] The three-parameter hybrid functional according to Becke with additional correlation corrections due to Lee, Yang, and Parr (B3LYP)[26,27] was utilized. The 6-311+G* basis set was used for the O atom, and the all-electron basis set of Wachters−Hay as modified by Gaussian was used for the Ti atom.[28] The SDD pseudopotential and basis set was used for the Zr and Hf atoms.[29] The geometries were fully optimized; the harmonic vibrational frequencies were calculated, and zero-point vibrational energies (ZPVE) were derived. For selected species, the single-point energies of the structures optimized at the B3LYP level of theory were calculated using the CCSD(T) method with the same basis sets.

Results and Discussion

Infrared Spectra. The reactions of laser-evaporated group IV metal atoms with oxygen in solid argon have been investigated previously, and the metal monoxide and dioxide molecules have been identified.[6] A series of experiments were performed with a wide range of O_2 concentrations and laser energies. The experiments with low O_2 concentrations and high laser energies are of particular interest here. The infrared spectra in the Ti−O stretching frequency region with 0.05% O_2 in argon

* Corresponding author. E-mail: mfzhou@fudan.edu.cn.

10.1021/jp0711388 CCC: $37.00
Published on Web 04/17/2007

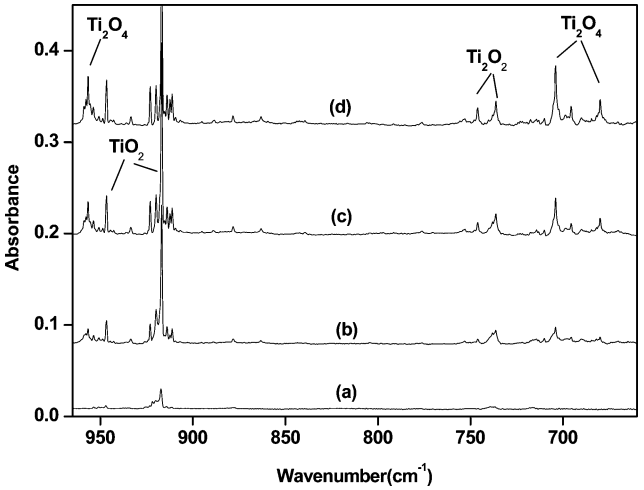

Figure 1. Infrared spectra in the 965−660 cm^{-1} region from co-deposition of laser-evaporated titanium atoms and clusters with 0.05% O_2 in argon: (a) 1 h of sample deposition at 6 K, (b) after 25 K annealing, (c) after 30 K annealing, and (d) after 35 K annealing.

TABLE 1: Infrared Absorptions (cm^{-1}) from Co-Deposition of Laser-Evaporated Titanium, Zirconium, and Hafnium Atoms with Dioxygen in Excess Argon

$^{16}O_2$	$^{18}O_2$	$^{16}O_2 + {}^{18}O_2$	$^{16}O_2 + {}^{16}O^{18}O + {}^{18}O_2$	assignment
746.1	713.9	746.1, 713.9	746.1, 740.8, 713.9	Ti_2O_2
736.2	704.6	736.2, 704.6	736.2, 710.0, 704.6	Ti_2O_2
956.8	916.7	968.0, 956.8, 924.2, 916.7	968.0, 956.8, 924.4, 916.7	Ti_2O_4
704.1	673.5	704.1, 689.5, 673.5	703.6, 689.4, 674.0	Ti_2O_4
695.7	665.8	695.7, 681.1, 665.8	695.6, 681.4, 665.9	Ti_2O_4 site
679.9	652.5	679.9, 659.5, 652.5	679.8, 659.5, 652.8	Ti_2O_4
701.5	666.4	701.5, 685.8, 666.4	684.2, 667.5, 648.7	Zr_2O_2
870.6	828.2	874.6, 870.6, 834.1, 828.2		Zr_2O_4
652.0	621.5	652.0, 637.8, 621.5	652.0, 637.8, 622.3	Zr_2O_4
643.7	613.5	643.7, 629.3, 613.5	643.0, 629.3, 613.5	Zr_2O_4 site
593.4	565.4	593.4, 575.2, 565.4	593.4, 575.2, 565.8	Zr_2O_4
684.2	648.7	684.2, 648.7	684.2, 667.5, 648.7	Hf_2O_2
866.4	820.8	868.8, 866.4, 824.3, 820.8		Hf_2O_4
651.1	617.6	651.1, 617.6		Hf_2O_4 site
649.4	616.1	649.4, 634.0, 616.1	648.4, 634.0, 616.6	Hf_2O_4
641.2	608.3	641.2, 626.2, 608.3	640.6, 626.2, 608.7	Hf_2O_4 site
593.3	562.6	593.3, 574.2, 562.6	593.2, 574.0, 562.7	Hf_2O_4 site
591.3	560.8	591.3, 572.4, 560.8	591.0, 572.4, 561.4	Hf_2O_4
583.3	553.2	583.3, 564.6, 553.2	582.9, 564.6, 553.8	Hf_2O_4 site

and approximately 8 mJ/pulse laser energy are shown in Figure 1, and the product absorptions are listed in Table 1. After sample deposition, absorptions of titanium dioxide at 946.6 (ν_1) and 917.0 cm^{-1} (ν_3) were observed,[6] which increased markedly upon sample annealing. Weak absorption of titanium monoxide at 987.9 cm^{-1} was also observed, but decreased upon sample annealing.[6] Besides the TiO and TiO_2 absorptions, two groups of new absorptions were produced. The 746.1 and 736.2 cm^{-1} absorptions are very weak upon sample deposition and increased together upon sample annealing. The 956.8, 704.1, and 679.9 cm^{-1} absorptions appeared on sample annealing to 25 K and increased together on 30 and 35 K annealing. Similar experiments were performed with the zirconium and hafnium metal targets. The resulting infrared spectra are shown in Figures 2 and 3, respectively. The new product absorptions are listed in Table 1. Besides the metal monoxide and dioxide absorptions, new absorptions at 701.5, 870.6, 652.0, and 593.4 cm^{-1} in the zirconium experiments and 684.2, 866.4, 649.4, and 591.3 cm^{-1} in the hafnium experiments were produced.

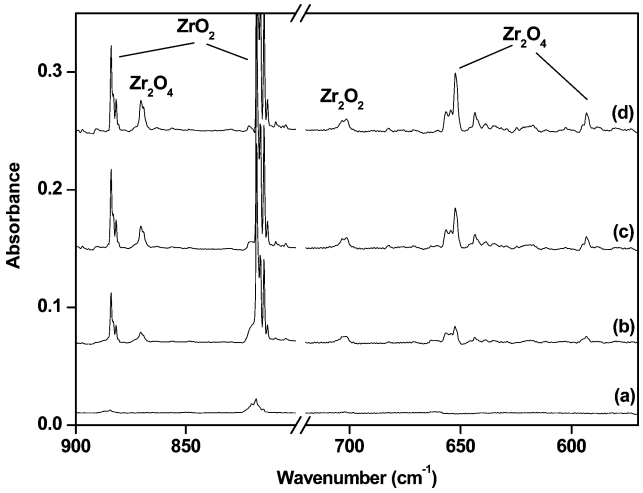

Figure 2. Infrared spectra in the 900−800 and 720−570 cm^{-1} regions from co-deposition of laser-evaporated zirconium atoms with 0.05% O_2 in argon: (a) 1 h of sample deposition at 6 K, (b) after 25 K annealing, (c) after 30 K annealing, and (d) after 35 K annealing.

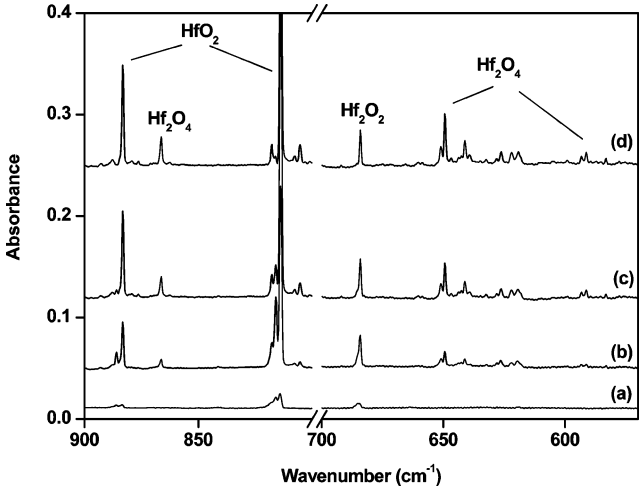

Figure 3. Infrared spectra in the 900−800 and 700−570 cm^{-1} regions from co-deposition of laser-evaporated hafnium atoms with 0.05% O_2 in argon: (a) 1 h of sample deposition at 6 K, (b) after 25 K annealing, (c) after 30 K annealing, and (d) after 35 K annealing.

The experiments were repeated by using the isotopically labeled $^{18}O_2$ sample and the $^{16}O_2 + {}^{18}O_2$ and $^{16}O_2 + {}^{16}O^{18}O + {}^{18}O_2$ mixtures. The spectra in selected regions with different isotopic samples are shown in Figures 4−6, respectively, with the isotopic counterparts summarized in Table 1.

M_2O_2. The absorptions at 746.1 and 736.2 cm^{-1} were only observed in the Ti + O_2 experiments with relatively high laser energy and low O_2 concentrations. These absorptions shifted to 713.9 and 704.6 cm^{-1} when the $^{18}O_2$ sample was used. The $^{16}O/^{18}O$ isotopic frequency ratios of 1.0451 and 1.0448 are very close to that of the diatomic Ti−O stretching. As shown in Figure 4, only the pure isotopic counterparts were observed in the experiment with the $^{16}O_2 + {}^{18}O_2$ mixed sample, while two intermediate absorptions at 740.8 and 710.0 cm^{-1} were produced in the experiment when the $^{16}O_2 + {}^{16}O^{18}O + {}^{18}O_2$ mixed sample was used. These spectral features indicate that two equivalent oxygen atoms, which arise from one O_2 molecule, are involved. The band positions and $^{16}O/^{18}O$ isotopic frequency ratios suggest the assignment to a cyclic Ti_2O_2 molecule.[6,30]

Quantum chemical calculations were performed to support the assignment. Calculations were performed on the singlet and triplet spin states of cyclic Ti_2O_2. Previous theoretical calculation

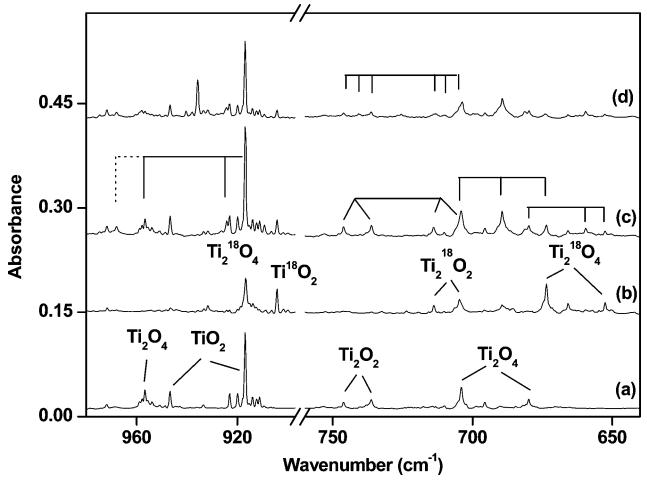

Figure 4. Infrared spectra in the 980−900 and 760−640 cm^{-1} regions from co-deposition of laser-evaporated titanium atoms with isotopic-labeled oxygen in excess argon. Spectra were taken after sample deposition followed by 35 K annealing: (a) 0.05% $^{16}O_2$, (b) 0.05% $^{18}O_2$, (c) 0.025% $^{16}O_2$ + 0.025% $^{18}O_2$, and (d) 0.0125% $^{16}O_2$ + 0.025% $^{16}O^{18}O$ + 0.0125% $^{18}O_2$.

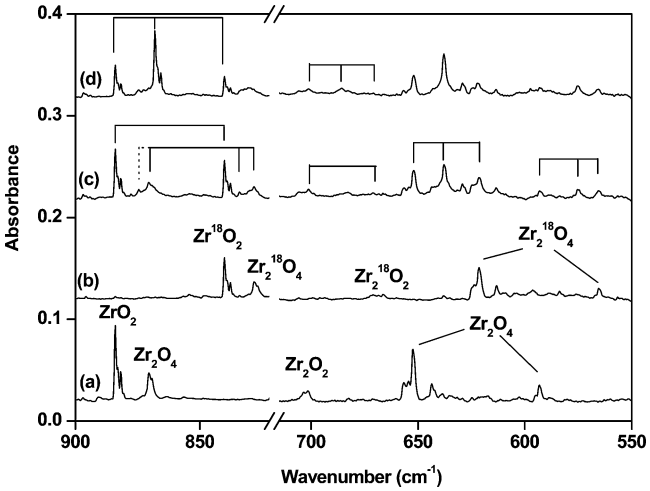

Figure 5. Infrared spectra in the 900−822 and 715−550 cm^{-1} regions from co-deposition of laser-evaporated zirconium atoms with isotopic-labeled oxygen in excess argon. Spectra were taken after sample deposition followed by 35 K annealing: (a) 0.05% $^{16}O_2$, (b) 0.05% $^{18}O_2$, (c) 0.025% $^{16}O_2$ + 0.025% $^{18}O_2$, and (d) 0.0125% $^{16}O_2$ + 0.025% $^{16}O^{18}O$ + 0.0125% $^{18}O_2$.

results suggest that the nonplanar structure is more stable than the planar structure.[19] At the DFT/B3LYP level of theory, both the singlet and triplet states were predicted to have a nonplanar C_{2v} structure and are very close in energy (Table 2). Therefore, additional single-point energy calculations were performed at the CCSD(T)/B3LYP level of theory. It was found that the singlet state is about 5.9 kcal/mol lower in energy than the triplet state. The singlet state Ti_2O_2 molecule was predicted to have two strong Ti−O stretching modes at 798.6 and 779.4 cm^{-1} with 74:241 km/mol relative IR intensities, which are in quite good agreement with the experimental observations. The calculated isotopic frequency ratios (Table 3) are also very close to the experimental values. These two modes for the triplet state were calculated at 735.8 and 718.3 cm^{-1}, too low to fit the experimental values. As shown in Figure 7, the $^1A_1$ ground state Ti_2O_2 molecule has a Ti−Ti distance of 2.136 Å, longer than the Ti−Ti quadruple bond of the $^3\Delta_g$ Ti_2 experimentally characterized (1.942 Å)[31] but shorter than the Ti−Ti double bond (2.326 Å) experimentally determined in the known

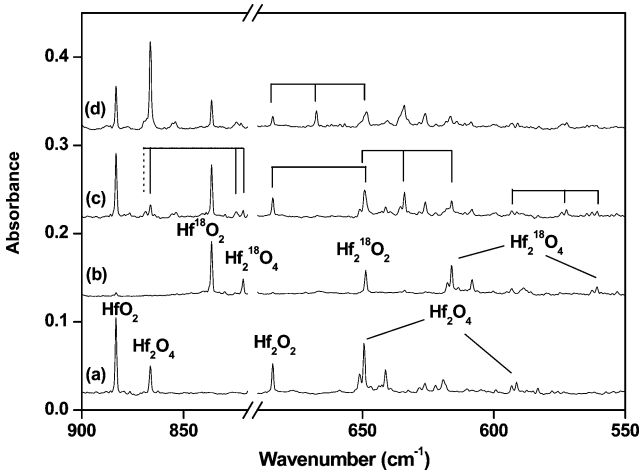

Figure 6. Infrared spectra in the 900−819 and 690−550 cm^{-1} regions from co-deposition of laser-evaporated hafnium atoms with isotopic-labeled oxygen in excess argon. Spectra were taken after sample deposition followed by 30 K annealing: (a) 0.1% $^{16}O_2$, (b) 0.1% $^{18}O_2$, (c) 0.05% $^{16}O_2$ + 0.05% $^{18}O_2$, and (d) 0.025% $^{16}O_2$ + 0.05% $^{16}O^{18}O$ + 0.025% $^{18}O_2$.

TABLE 2: DFT/B3LYP Calculated Total Energies (in Hartree, after Zero-Point Energy Corrections, the Values in Parentheses Are Single-Point Energies Calculated at the CCSD(T) Level), Frequencies (cm^{-1}), and Intensities (km/mol) of the M_2O_2 and M_2O_4 (M = Ti, Zr, Hf) Clusters

molecule	energy	frequency (intensity)
$Ti_2O_2(^3B_1)$	−1849.480466 (−1847.261419)	245.7(14), 322.4(0), 369.3(1), 472.4(0), 718.3(195), 735.8(61)
$Ti_2O_2(^1A_1)$	−1849.479820 (−1847.270820)	296.0(2), 349.2(0), 439.9(3), 445.7(51), 779.4(241), 798.6(74)
$Zr_2O_2(^1A_g)$	−244.637464 (−243.694921)	140.3(9), 311.1(0), 466.0(0), 604.2(49), 674.7(282), 691.9(0)
$Zr_2O_2(^1A_1)$	−244.642178 (−243.662436)	275.4(4), 301.5(0), 316.8(27), 376.8(0), 680.8(179), 705.6(95)
$Zr_2O_2(^3B_1)$	−244.643904 (−243.668886)	230.4(12), 307.9(0), 316.6(0), 437.4(92), 646.1(109), 669.5(33)
$Hf_2O_2(^1A_g)$	−246.599222	185.7(5), 217.5(0), 449.3(0), 572.8(37), 663.0(300), 684.5(0)
$Ti_2O_4(^1A_g)$	−2000.174538	92.0(41), 184.4(23), 189.9(0), 284.3(0), 340.7(68), 410.8(0), 487.7(0), 687.8(224), 726.3(606), 727.6(0), 1021.1(644), 1041.9(0)
$Zr_2O_4(^1A_g)$	−395.344564	80.2(48), 163.0(0), 166.0(34), 266.0(0), 307.7(0), 314.6(48), 463.0(0), 589.4(206), 657.9(0), 670.5(640), 890.0(424), 900.4(0)
$Hf_2O_4(^1A_g)$	−397.263892	69.7(49), 151.9(0), 172.4(36), 228.5(0), 265.8(0), 305.2(36), 485.3(0), 563.5(169), 643.1(0), 656.0(569), 864.3(306), 871.5(0)

compound bis(μ-η^5:η^5-1,4-bis(trimethylsilyl)cyclo-octatetraene) dititanium.[32] The separation between the two oxygen atoms was computed to be 2.764 Å , indicating that there is no direct bonding interaction between the two O atoms.

In the zirconium experiments, the 701.5 cm^{-1} absorption exhibits similar behavior as the cyclic Ti_2O_2 absorptions. This absorption was produced only in the experiments with high laser energies and low O_2 concentrations. It shifted to 666.4 cm^{-1} with $^{18}O_2$, giving an $^{16}O/^{18}O$ isotopic frequency ratio of 1.0527. The spectra with the $^{16}O_2$ + $^{18}O_2$ and $^{16}O_2$ + $^{16}O^{18}O$ + $^{18}O_2$ mixtures shown in Figure 5 clearly indicate that two equivalent oxygen atoms are involved in this mode. Accordingly, we assign the 701.5 cm^{-1} absorption to the cyclic Zr_2O_2 molecule. DFT/B3LYP calculations were performed on the singlet and triplet spin states of Zr_2O_2 with cyclic structures, and the results are summarized in Table 2. In the singlet potential energy surface,

TABLE 3: Comparisons between the Calculated and Experimentally Observed Vibrational Frequencies (cm^{-1}) and Isotopic Frequency Ratios of the M_2O_2 and M_2O_4 Clusters

		frequency		$^{16}O/^{18}O$	
molecule	mode	calcd	obsd	calcd	obsd
Ti_2O_2	a_1	798.6	746.1	1.0443	1.0451
	b_2	779.4	736.2	1.0466	1.0448
Zr_2O_2	b_{1u}	674.7	701.5	1.0509	1.0527
Hf_2O_2	b_{1u}	663.0	684.2	1.0554	1.0547
Ti_2O_4	b_u (asym Ti═O str.)	1021.1	956.8	1.0444	1.0437
	b_u (Ti−O str.)	726.3	704.1	1.0452	1.0454
	a_u (Ti−O str.)	687.8	679.9	1.0423	1.0420
Zr_2O_4	b_u (asym Zr═O str.)	890.0	870.6	1.0511	1.0512
	b_u (Zr−O str.)	670.5	652.0	1.0501	1.0491
	a_u (Zr−O str.)	589.4	593.4	1.0495	1.0495
Hf_2O_4	b_u (asym Hf═O str.)	864.3	866.4	1.0557	1.0556
	b_u (Hf−O str.)	656.0	649.4	1.0547	1.0540
	a_u (Hf−O str.)	563.5	591.3	1.0547	1.0544

both the planar D_{2h} structure and the nonplanar C_{2v} structure are local minima, with the nonplanar structure slightly lower in energy than the planar structure. The lowest triplet state was predicted to be nonplanar and is 1.0 kcal/mol more stable than the nonplanar singlet state. At the CCSD(T)/B3LYP level of theory, the planar singlet state (^1A_g) was predicted to be the ground state. The nonplanar singlet and triplet states lie about 20.4 and 16.3 kcal/mol above the planar singlet state. The ^1A_g state Zr_2O_2 molecule was calculated to have a strong Zr−O stretching mode at 674.7 cm^{-1}, slightly lower than the observed values. Similar planar cyclic structures have been observed for the recently reported Co_2O_2 and Ni_2O_2 molecules.[33,34] The Zr−Zr distance of the ^1A_g ground state Zr_2O_2 molecule was estimated to be 2.963 Å, slightly shorter that the experimentally characterized Zr−Zr single bond.[35]

The 684.2 cm^{-1} absorption in the Hf + O_2 reaction is assigned to the cyclic Hf_2O_2 molecule following the example of Ti_2O_2 and Zr_2O_2. The DFT/B3LYP calculations predicted that the Hf_2O_2 molecule has a ^1A_g ground state (Figure 7) and a planar cyclic structure with D_{2h} symmetry. The lowest triplet state was predicted to lie 13.0 kcal/mol higher in energy than the singlet ground state. The observed mode was computed at 663.0 cm^{-1}, with the isotopic frequency ratio in excellent agreement with the experimental value (Table 3).

The M−O stretching vibrational frequencies of M_2O_2 decrease from Ti to Hf, similar to the trend for the M−O stretching frequencies of the monoxides and dioxides.[6] The Ti_2O_2 molecule is nonplanar with a strong Ti−Ti bond, while the Zr_2O_2 and Hf_2O_2 clusters have a planar structure.

M_2O_4. The absorptions at 956.8, 704.1, and 679.5 cm^{-1} were previously observed from co-deposition of laser-ablated titanium and oxygen in solid argon.[6] The 958.6 cm^{-1} absorption was tentatively assigned to a Ti_2O_3 cluster. The 704.1 and 679.9 cm^{-1} absorptions correspond to the absorptions reported at 704.2 and 680.1 cm^{-1} that were tentatively assigned to the cyclic Ti_2O_2 molecule.[6] The present experiments provide strong evidence that these three absorptions remain constant relative IR intensities throughout all the experiments, indicating that they are due to different vibrational modes of the same molecule. In agreement with a previous report,[6] the 704.1 and 679.9 cm^{-1} absorptions are due to the vibrational modes of a cyclic Ti_2O_2 unit. These absorptions shifted to 673.5 and 652.5 cm^{-1} with $^{18}O_2$, giving the $^{16}O/^{18}O$ isotopic frequency ratios of 1.0454 and 1.0420, respectively, which are diatomic Ti−O stretching frequency ratios. As shown in Figure 4, both absorptions split into a triplet in the mixed $^{16}O_2$ + $^{18}O_2$ (Figure 4, trace c) and

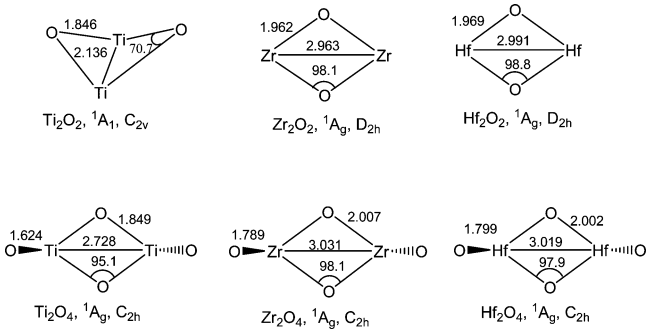

Figure 7. Optimized geometric parameters (bond lengths in Å and bond angles in deg) of the M_2O_2 and M_2O_4 clusters.

$^{16}O_2$ + $^{16}O^{18}O$ + $^{18}O_2$ (Figure 4, trace d) spectra, indicating that two equivalent O atoms are involved in these two modes. The mixed isotopic spectral features also indicate that the two oxygen atoms arise from two different oxygen molecules. It is important to note that the peak positions in the mixed $^{16}O_2$ + $^{16}O^{18}O$ + $^{18}O_2$ experiment are slightly shifted from those in the pure and mixed $^{16}O_2$ + $^{18}O_2$ experiments, which suggest that both modes were slightly perturbed by other O atom(s), therefore, the 704.1 and 679.9 cm^{-1} absorptions are not due to isolated Ti_2O_2 molecule. The 956.8 cm^{-1} absorption shifted to 916.7 cm^{-1} when an $^{18}O_2$ sample was used. The band position and the $^{16}O/^{18}O$ isotopic frequency ratio of 1.0437 suggest that this absorption is due to a terminal Ti═O stretching vibration. In the mixed $^{16}O_2$ + $^{18}O_2$ spectrum (Figure 4, trace c), the $^{18}O_2$ counterpart was overlapped by the strong antisymmetric stretching mode of TiO_2, but two intermediate absorptions at 968.0 and 924.2 cm^{-1} were clearly resolved. This spectral feature implies that this mode involves two equivalent Ti═O subunits. The observation of only one Ti═O stretching mode suggests that the molecule is centrosymmetric. The above-mentioned experimental observations suggest that the assignment of the 956.8, 704.1, and 679.9 cm^{-1} absorptions to a planar OTi(μ-O)$_2$TiO cluster. The 956.8 cm^{-1} absorption is due to the antisymmetric Ti═O stretching mode. The symmetric stretching mode for centrosymmetric Ti_2O_4 is IR inactive, but this mode of partially substituted ^{16}OTi(μ-O)$_2$Ti^{18}O is IR active because of the reduced symmetry. The 968.0 cm^{-1} absorption observed in the mixed $^{16}O_2$ + $^{18}O_2$ spectrum is due to the symmetric mode of ^{16}OTi(μ-O)$_2$Ti^{18}O.

The geometry of Ti_2O_4 was calculated previously.[7,17,20,21] These calculations predicted that the Ti_2O_4 cluster has an ^1A_g ground state with a nonplanar C_{2h} symmetry. Similar results were obtained in the present study at the DFT/B3LYP level of theory. As shown in Figure 7, the molecule involves a rhombus Ti(μ-O)$_2$Ti subunit and two terminal O atoms bending out of the Ti(μ-O)$_2$Ti plane in opposite directions. The two terminal Ti═O bonds were predicted to have a bond length of 1.624 Å, slightly longer than that of diatomic TiO molecule (1.612 Å) calculated at the same level of theory. The Ti−O bond length of the cyclic subunit is computed to be 1.849 Å, about the same as that of the cyclic Ti_2O_2 molecule. However, the Ti−Ti distance (2.728 Å) is much longer than that of the cyclic Ti_2O_2 molecule (2.136 Å). The three experimentally observed vibrational modes were computed to absorb at 1021.1, 726.3, and 687.8 cm^{-1} with 644:606:224 km/mol relative IR intensities. As listed in Table 3, the calculated isotopic frequency ratios are also in very good agreement with the experimental values.

In the experiments with zirconium, similar absorptions at 870.6, 652.0, and 593.4 cm^{-1} are assigned to the Zr_2O_4 molecule. The 870.6 cm^{-1} absorption is a terminal Zr═O stretching mode with a $^{16}O/^{18}O$ ratio of 1.0502. The 652.0 and

593.4 cm^{-1} absorptions belong to the Zr−O stretching modes of the cyclic Zr(μ-O)$_2$Zr subunit. As shown in Figure 7, DFT/B3LYP calculations predicted that the Zr_2O_4 molecule has an ^1A_g ground state with a nonplanar C_{2h} symmetry, which is consistent with previous calculations.[13,21,22] The three experimentally observed vibration modes were predicted at 890.0, 670.5, and 589.4 cm^{-1}, with the isotopic frequency ratios very close to the observed values (Table 3).

The absorptions at 866.4, 649.4, and 591.3 cm^{-1} in the reaction of hafnium atoms with dioxygen are assigned to different vibrational modes of the Hf_2O_4 molecule, which also was predicted to have a ^1A_g ground state with C_{2h} symmetry. The match between the observed and calculated vibrational frequencies and isotopic frequency ratios (Table 3) confirms the assignment.

Reaction Mechanism. The experimental observations demonstrate that the M_2O_2 molecules were formed by the reactions of metal dimer and oxygen in solid argon, reactions 1−3. There is no bonding interaction between the two O atoms in M_2O_2, indicating that the O−O bond is completely cleaved. The M_2O_2 absorptions increased on sample annealing, suggesting that the O−O bond dissociation reactions 1−3 are exothermic and proceed with negligible activation energy. Recent investigations indicate that the Ti dimer reacted with N_2 to form a N−N bond completely cleavaged cyclic Ti(μ-N)$_2$Ti molecule in a single step without a significant activation barrier.[30] The metal monoxides were also produced during sample deposition, the M_2O_2 molecules may also be formed from MO dimerization reactions, which were predicted to be exothermic (exothermic by 57.9, 77.0, and 65.9 kcal/mol for Ti, Zr, and Hf, respectively). However, our experimental observations indicate that the dimerization reaction channel was not observed. If the M_2O_2 molecules were produced from MO dimerization, intermediate absorptions due to $M_2{}^{16}O^{18}O$ should be observed in the experiment when the $^{16}O_2 + {}^{18}O_2$ mixed sample was used.

$$Ti_2\,(^3\Delta_g) + O_2\,(^3\Sigma_g) \rightarrow Ti_2O_2\,(^1A_1) \qquad \Delta E = -228.0 \text{ kcal/mol} \quad (1)$$

$$Zr_2\,(^3\Delta_g) + O_2\,(^3\Sigma_g) \rightarrow Zr_2O_2\,(^1A_g) \qquad \Delta E = -234.3 \text{ kcal/mol} \quad (2)$$

$$Hf_2\,(^3\Sigma_u) + O_2\,(^3\Sigma_g) \rightarrow Hf_2O_2\,(^1A_g) \qquad \Delta E = -270.4 \text{ kcal/mol} \quad (3)$$

The M_2O_4 molecules were produced by the dimerization reaction between two metal dioxide molecules, reactions 4−6. The experimental observations indicate that these dimerization reactions proceed spontaneously and require negligible activation energy. The dimerization reactions were predicted to be strongly exothermic.

$$2TiO_2\,(^1A_1) \rightarrow Ti_2O_4\,(^1A_g) \qquad \Delta E = -110.6 \text{ kcal/mol} \quad (4)$$

$$2ZrO_2\,(^1A_1) \rightarrow Zr_2O_4\,(^1A_g) \qquad \Delta E = -122.3 \text{ kcal/mol} \quad (5)$$

$$2HfO_2\,(^1A_1) \rightarrow Hf_2O_4\,(^1A_g) \qquad \Delta E = -138.8 \text{ kcal/mol} \quad (6)$$

Conclusions

The reactions of group IV metal atoms and dimers with molecular oxygen were investigated in solid argon. The reaction product absorptions were identified on the basis of isotopic substitution and quantum chemical theoretical calculations. Besides the previously characterized metal monoxide and dioxide molecules, dinuclear metal oxide clusters, M_2O_2 and M_2O_4 (M = Ti, Zr, Hf) were produced by co-deposition of laser-evaporated group IV metal atoms and dimers using relatively low O_2 concentrations and high laser energy. The M_2O_2 clusters were formed through the reactions of metal dimers and O_2 in a single step without significant activation barrier in solid argon. The results show that the Ti_2O_2 cluster has a singlet ground state with a nonplanar cyclic C_{2v} structure with a strong Ti−Ti bond, while the Zr_2O_2 and Hf_2O_2 clusters have planar cyclic structures. The M_2O_4 clusters were characterized to have a closed-shell singlet ground state with a nonplanar C_{2h} symmetry. The M_2O_4 clusters were formed from the dimerization of the metal dioxide molecules which require negligible activation energy. The M_2O_2 and M_2O_4 (M = Ti, Zr, Hf) clusters are fundamental building blocks for the formation of larger metal oxide clusters.

Acknowledgment. We gratefully acknowledge financial support from National Natural Science Foundation (grant no. 20433080) and the Ministry of Science and Technology (2004CB719501) of China.

References and Notes

(1) See for example: (a) Fernández, P.; Blanco, J.; Sichel, C.; Malato, S. *Catal. Today* **2005**, *101*, 345. (b) Pozzo, R.; Baltanás, M.; Cassano, A. *Catal. Today* **1997**, *39*, 219. (c) Yamaguchi, T. *Catal. Today* **1994**, *20*, 199.

(2) Huber, K. P.; Herzberg, G. *Constants of Diatomic Molecules*: Van Nostrand Reinhold: New York, 1979.

(3) McIntyre, N. S.; Thompson, K. R.; Weltner, W., Jr. *J. Phys. Chem.* **1971**, *75*, 3243.

(4) Kaufman, M.; Muenter, J.; Klemperer, W. *J. Chem. Phys.* **1967**, *47*, 3365.

(5) Gallaher, T. N.; DeVore, T. C. *High Temp. Sci.* **1983**, *16*, 269.

(6) Chertihin, G. V.; Andrews, L. *J. Phys. Chem.* **1995**, *99*, 6356.

(7) Wu, H. B.; Wang, L. S. *J. Chem. Phys.* **1997**, *107*, 8221.

(8) (a) Thomas, O. C.; Xu, S. J.; Lippa, T. P.; Bowen, K. H. *J. Cluster Sci.* **1999**, *10*, 525. (b) Zheng, W. J.; Bowen, K. H.; Li, J.; Dabkowska, I.; Gutowski, M. *J. Phys. Chem. A* **2005**, *109*, 11521.

(9) (a) Brugh, D. J.; Suenram, R. D.; Stevens, W. J. *J. Chem. Phys.* **1999**, *111*, 3526. (b) Lesarri, A.; Suenram, R. D.; Brugh, D. J. *J. Chem. Phys.* **2002**, *117*, 9651.

(10) Matsuda, Y.; Bernstein, E. R. *J. Phys. Chem. A* **2005**, *109*, 314.

(11) (a) Foltin, M.; Stueber, G. J.; Bernstein. E. R. *J. Chem. Phys.* **2001**, *114*, 8971. (b) Matsuda,Y.; Shin, D. N.; Bernstein, E. R. *J. Chem. Phys.* **2004**, *120*, 4142.

(12) Demyk, K.; van Heijnsbergen, D.; von Helden, G.; Meijer, G. *Astron. Astrophys.* **2004**, *420*, 547.

(13) von Helden, G.; Kirilyuk, A.; van Heijnsbergen, D.; Sartakov, B.; Duncan, M. A.; Meijer, G. *Chem. Phys.* **2000**, *262*, 31.

(14) Hagfeldt, A.; Bergstrom, R.; Siegbahn, H. O. G.; Lunell, S. *J. Phys. Chem.* **1993**, *97*, 12725.

(15) Walsh, M. B.; King, R. A.; Schaefer, H. F. *J. Chem. Phys.* **1999**, *110*, 5224.

(16) Tsipis, A. C.; Tsipis, C. A. *Phys. Chem. Chem. Phys.* **1999**, *1*, 4453.

(17) Albaret, T.; Finocchi, F.; Noguera, C. *J. Chem. Phys.* **2000**, *113*, 2238.

(18) Jeong, K. S.; Chang, C.; Sedlmayr, E.; Sulzle, D. *J. Phys. B* **2000**, *33*, 3417.

(19) Xiang, J.; Yan, X. H.; Xiao, Y.; Mao, Y. L.; Wei, S. H. *Chem. Phys. Lett.* **2004**, *387*, 66.

(20) Qu, Z. W.; Kroes, G. J. *J. Phys. Chem. B* **2006**, *110*, 8998.

(21) Woodley, S. M.; Hamad, S.; Mejías, J. A.; Catlow, C. R. A. *J. Mater. Chem.* **2006**, *16*, 1927. Hamad, S.; Catlow, C. R. A.; Woodley, S. M.; Lago, S.; Mejías, J. A. *J. Phys. Chem. B* **2005**, *109*, 15741.

(22) Chen, S. G.; Yin, Y. S.; Wang, D. P.; Liu, Y. C.; Wang, X. *J. Cryst. Growth* **2005**, *282*, 498.

(23) (a) Wang, G. J.; Gong, Y.; Chen, M. H.; Zhou, M. F. *J. Am. Chem. Soc.* **2006**, *128*, 5974. (b) Miao, L.; Dong, J.; Yu, L.; Zhou, M. F. *J. Phys. Chem. A* **2003**, *107*, 1935. (c) Shao, L. M.; Zhang, L. N.; Chen, M. H.; Lu, H.; Zhou, M. F. *Chem. Phys. Lett.* **2001**, *343*, 178.

(24) (a) Zhou, M. F.; Jin, X.; Li, J. *J. Phys. Chem. A* **2006**, *110*, 10206. (b) Chen, M. H.; Wang, X. F.; Zhang, L. N.; Yu, M.; Qin, Q. Z. *Chem. Phys.* **1999**, *242*, 81.

(25) Frisch, M. J.; Trucks, G. W.; Schlegel, H. B.; Scuseria, G. E.; Robb, M. A.; Cheeseman, J. R.; Montgomery, J. A., Jr.; Vreven, T.; Kudin, K. N.; Burant, J. C.; Millam, J. M.; Iyengar, S. S.; Tomasi, J.; Barone, V.; Mennucci, B.; Cossi, M.; Scalmani, G.; Rega, N.; Petersson, G. A.; Nakatsuji, H.; Hada, M.; Ehara, M.; Toyota, K.; Fukuda, R.; Hasegawa, J.; Ishida, M.; Nakajima, T.; Honda, Y.; Kitao, O.; Nakai, H.; Klene, M.; Li, X.; Knox, J. E.; Hratchian, H. P.; Cross, J. B.; Bakken, V.; Adamo, C.; Jaramillo, J.; Gomperts, R.; Stratmann, R. E.; Yazyev, O.; Austin, A. J.; Cammi, R.; Pomelli, C.; Ochterski, J. W.; Ayala, P. Y.; Morokuma, K.; Voth, G. A.; Salvador, P.; Dannenberg, J. J.; Zakrzewski, V. G.; Dapprich, S.; Daniels, A. D.; Strain, M. C.; Farkas, O.; Malick, D. K.; Rabuck, A. D.; Raghavachari, K.; Foresman, J. B.; Ortiz, J. V.; Cui, Q.; Baboul, A. G.; Clifford, S.; Cioslowski, J.; Stefanov, B. B.; Liu, G.; Liashenko, A.; Piskorz, P.; Komaromi, I.; Martin, R. L.; Fox, D. J.; Keith, T.; Al-Laham, M. A.; Peng, C. Y.; Nanayakkara, A.; Challacombe, M.; Gill, P. M. W.; Johnson, B.; Chen, W.; Wong, M. W.; Gonzalez, C.; Pople, J. A. *Gaussian 03*, revision B.05; Gaussian, Inc.: Wallingford, CT, 2004.

(26) Becke, A. D. *J. Chem. Phys.* **1993**, *98*, 5648.

(27) Lee, C.; Yang, W.; Parr, R. G. *Phys. Rev. B* **1988**, *37*, 785.

(28) (a) McLean, A. D.; Chandler, G. S. *J. Chem. Phys.* **1980**, *72*, 5639. (b) Krishnan, R.; Binkley, J. S.; Seeger, R.; Pople, J. A. *J. Chem. Phys.* **1980**, *72*, 650.

(29) (a) Dolg, M.; Stoll, H.; Preuss, H. *J. Chem. Phys.* **1989**, *90*, 1730. (b) Andrae, D.; Haussermann, U.; Dolg, M.; Stoll, H.; Preuss, H. *Theor. Chim. Acta* **1990**, *77*, 123.

(30) (a) Himmel, H. J.; Hübner, O.; Klopper, W.; Manceron, L. *Angew. Chem., Int. Ed.* **2006**, *45*, 2799. (b) Himmel, H. J.; Hübner, O.; Bischoff, F. A.; Klopper, W.; Manceron, L. *Phys. Chem. Chem. Phys.* **2006**, *8*, 2000.

(31) Doverstal, M.; Lindgren, B.; Sassenberg, U.; Arrington, C. A.; Morse, M. D. *J. Chem. Phys.* **1992**, *97*, 7087.

(32) Horáček, M.; Kupfer, V.; Thewalt, U.; Štěpnička, P.; Polášek, M.; Mach, K. *J. Organomet. Chem.* **1999**, *584*, 286.

(33) Danset, D.; Manceron, L. *Phys. Chem. Chem. Phys.* **2005**, *7*, 583.

(34) Allouti, F.; Manceron, L.; Alikhani, M. E. *Phys. Chem. Chem. Phys.* **2006**, *8*, 3715.

(35) Cotton, F. A.; Diebold, M. P.; Kibala, P. A. *Inorg. Chem.* **1988**, *27*, 799.